# Histone deacetylase 4 deletion results in abnormal chondrocyte hypertrophy and premature ossification from collagen type 2α1-expressing cells

GUOQING DU[1,2*], CHUAN XIANG[3*], XIAOWEN SANG[1*], XIANG WANG[1], YING SHI[1], NAN WANG[1], SHAOWEI WANG[3], PENGCUI LI[3], XIAOCHUN WEI[3], MIN ZHANG[1], LILAN GAO[4], HONGSHENG ZHAN[1] and LEI WEI[2]

[1]Shi's Center of Orthopedics and Traumatology, Shuguang Hospital Affiliated to Shanghai University of Traditional Chinese Medicine (TCM), Institute of Traumatology and Orthopedics, Shanghai Academy of TCM, Shanghai 201203, P.R. China; [2]Department of Orthopedics, The Warren Alpert Medical School of Brown University and Rhode Island Hospital, Providence, RI 02903, USA; [3]Department of Orthopedics, The Second Hospital Shanxi Medical University, Taiyuan, Shanxi 030001; [4]Tianjin Key Laboratory for Control Theory and Applications in Complicated Industry Systems, School of Mechanical Engineering, Tianjin University of Technology, Tianjin 300384, P.R. China

Received May 22, 2019; Accepted July 29, 2020

DOI: 10.3892/mmr.2020.11465

**Abstract.** Histone deacetylase 4 (HDAC4) plays a vital role in chondrocyte hypertrophy and bone formation. To investigate the function of HDAC4 in postnatal skeletal development, the present study developed lineage-specific *HDAC4*-knockout mice [collagen type 2α1 (Col2α1)-Cre, HDAC4$^{d/d}$ mice] by crossing transgenic mice expressing Cre recombinase. Thus, a specific ablation of HDAC4 was performed in Col2α1-expressing mice cells. The knee joints of HDAC4$^{fl/fl}$ and Col2α1-Cre, HDAC4$^{d/d}$ mice were analyzed at postnatal day (P)2-P21 using an *in vivo* bromodeoxyuridine (BrdU) assay, and Safranin O, Von Kossa and whole-body staining were used to evaluate the developmental growth plate, hypertrophic differentiation, mineralization and skeletal mineralization patterns. The trabecular bone was analyzed using microcomputed tomography. The expressions of BrdU, proliferating cell nuclear antigen (PCNA), matrix metalloproteinase (MMP)-13, runt-related transcription factor (Runx)-2, osteoprotegerin (OPG), CD34, type X collagen (ColX), osteocalcin and Wnt5a were determined using immunohistochemistry, *in situ* hybridization (ISH) and reverse transcription-quantitative (RT-q)PCR. The results demonstrated that HDAC4-null mice (HDAC4$^{d/d}$ mice) were severely runted; these mice had a shortened hypertrophic zone (histopathological evaluation), accelerated vascular invasion and articular mineralization (Von Kossa staining), elevated expressions of MMP-13, Runx2, OPG and CD34 (RT-qPCR and immunohistochemistry), downregulated expression of the proliferative marker BrdU and PCNA (immunohistochemistry), increased expression of ColX and decreased expression of Wnt5a (ISH). In conclusion, chondrocyte-derived HDAC4 was responsible for regulating chondrocyte proliferation and differentiation as well as endochondral bone formation.

*Correspondence to:* Professor Lei Wei, Department of Orthopedics, The Warren Alpert Medical School of Brown University and Rhode Island Hospital, Suite 402A, 1 Hoppin Street, Providence, RI 02903, USA
E-mail: lei_wei@brown.edu

Professor Hongsheng Zhan, Shi's Center of Orthopedics and Traumatology, Shuguang Hospital Affiliated to Shanghai University of Traditional Chinese Medicine (TCM), Institute of Traumatology and Orthopedics, Shanghai Academy of TCM, Suite 109, 528 Zhangheng Street, Shanghai 201203, P.R. China
E-mail: zhanhongsheng2010@163.com

*Contributed equally

*Abbreviations:* ISH, *in situ* hybridization; PBS, phosphate-buffered saline; HDAC4, histone deacetylase 4

*Key words:* HDAC4, chondrocyte hypertrophy, premature ossification

## Introduction

Chondrocyte differentiation is a pivotal event during bone formation in most mammals, and it comprises of two processes (1). Intramembranous ossification is an essential process during which mesenchymal stem cells directly differentiate into osteoblasts and is responsible for the development of irregular bones, such as the skull bone, clavicle and parts of the jaw (1). Endochondral ossification is the second important process of chondrocyte differentiation, responsible for the formation of long bones and vertebrate skeleton (2), which is controlled by a series of events (3). These events are initiated by the establishment of a chondrogenic template and culminated by its replacement with the coordinated activity of osteoblasts,

osteoclasts and endothelial cells (3,4). Chondrocyte maturation ultimately leads to hypertrophy, which is an essential contributor to longitudinal bone growth (5,6). However, abnormal chondrocyte hypertrophy is involved in the pathogenesis of osteoarthritis and skeletal dysplasia (7). Meanwhile, histone deacetylase 4 (HDAC4) is known as a member of a large family of HDAC that alter gene expression by catalyzing the removal of acetyl groups from core histones, which are responsible for chondrocyte hypertrophy and bone formation (8,9). However, the regulatory mechanism underpinning HDAC4 function remains largely unclear. Therefore, a better understanding of the mechanism underlying HDAC4-mediated regulation of endochondral ossification in chondrocyte hypertrophy is necessary for the improved management of skeletal growth diseases.

A previous study demonstrated that HADC4 plays an important role in the formation of the skeletal system (10). Knockout of HDAC4, a repressor of matrix metalloproteinase-13 (MMP-13) transcription, results in increased MMP-13 expression *in vitro* and *in vivo* (11). MMP-13 plays a critical role in endochondral ossification and bone remodeling (12). Chen *et al* (13) reported that HDAC4 inhibits the expression of MMP-13 and prevents chondrocyte hypertrophy by inhibiting the activity of runt-related transcription factor-2 (Runx2), a transcription factor essential during endochondral bone formation. Wnt5a is a secreted glycoprotein belonging to the Wingless/integrase 1 family of secreted glycoproteins; it is highly conserved among species and plays key roles in processes regulating embryonic development and postnatal tissue homeostasis (14). *Wnt5a*-knockout mice reportedly demonstrate perinatal lethality primarily due to respiratory failure and present extensive developmental abnormalities and the *Wnt5a* signaling pathway can regulate fundamental cellular processes, including cell proliferation and survival (15). Therefore, HDAC4 is considered as a central regulator of chondrocyte hypertrophy and growth plate development, and the complete deletion of HDAC4 is lethal (9,10,16-18). To investigate the roles of HDAC4 in postnatal skeletal development, the present study constructed a mouse strain with conditional *HDAC4*-knockout in collagen type 2α1 (Col2α1)-expressing cells.

## Materials and methods

*Generation of floxed HDAC4 animals*. The animal experiments and protocol were approved by the Institutional Animal Care and Use Committee of Rhode Island Hospital (Providence, United States of America). To investigate the physiological role of HDAC4 in hypertrophic chondrocytes, the *HDAC4* gene was deleted in Col2α1-Cre mice using the Cre/loxP gene targeting technique (six female mice, mean weight 20 g, from University of Texas Southwestern Medical Center, mice transgenic for Cre in Col2α1-expressing chondrocytes). Col2α1-Cre mice were mated with $HDAC4^{fl/fl}$ (six male mice, mean weight 20 g, provided by Dr Olson, University of Texas Southwestern Medical Center) animals to obtain $HDAC4^{fl/-}$, Col2α1-Cre mice (9). Mice transgenic for Cre in Col2α1-expressing chondrocytes (Col2α1-Cre) have been previously reported (19). These mice were subsequently interbred with $HDAC4^{fl/fl}$ animals, and their offspring ($HDAC4^{d/d}$, Col2α1-Cre) and $HDAC4^{fl/fl}$ animals were analyzed at postnatal (P) days 2, 4, 6, 8, 10 and 21 after birth. All mice were housed in a cage with free access to tap water and food. The housing environment was set at 22±2˚C and 60±10% humidity in a 12-h light/dark cycle. The health and behavior of mice were monitored and recorded on a daily basis. A total of 40 mice were divided into two groups ($HDAC4^{fl/fl}$ group and $HDAC4^{d/d}$; Col2α1-Cre group; n=20 for each group). The mice were euthanized by an overdose of carbon dioxide according to the American Veterinary Medical Association (AVMA) guidelines (20). The experiment endpoint was set when mice were postnatal 21 days old. The mice are first put into the euthanasia chamber and $CO_2$ was directed into the top of the euthanasia chamber. Weep holes were drilled into the euthanasia chamber lid to allow room air to escape as $CO_2$ filled the chamber. One-hundred percent compressed $CO_2$ gas was used to euthanize mice. When the flow rate displaced no ≤30% of the chamber volume/minute for apparent death, death was confirmed by absence of breathing or heartbeat. In this way, the mice had no pain, no nerve reaction and no signs of bleeding. The growth progress of mice was recorded at postnatal (P) days 2, 4, 6 and 8, 10 and 21.

*Genotyping and PCR*. Genomic DNA was isolated from skin tissue from the tail of the mice using the QIAamp DNA Micro kit (Qiagen GmbH) and used for PCR genotype identification of $HDAC4^{d/d}$, Col2α1-Cre transgenic mice. Routine mouse genotyping was performed using PCR, using the DNA polymerase Hotstar from Qiagen GmbH. The following primer pairs were used for the Cre allele: Forward, 5'-ATCCGAAAAGAAAAC GTTGA-3' and reverse, 5'-ATCCAGGTTACGGATATAGT-3'. PCR was initiated for 15 min at 95˚C, then 30 cycles of denaturation at 95˚C for 30 sec, primer annealing for 40 sec at 55˚C and a final extension step at 72˚C for 1 min. The *HDAC4* allele and target gene deletion were identified using the following primers: Forward, 5'-ATCTGCCCACCAGAGTATGTG-3' and reverse, 5'-CTTGTTGAGAACAAACTCCTGCAG CT-3'. PCR was initiated for 15 min at 95˚C, then 35 cycles of denaturation at 94˚C for 40 sec, primer annealing for 40 sec at 58.5˚C and a final extension step at 72˚C for 1 min. The expected product sizes for the wild-type *HDAC4*, floxed and Cre alleles were 480, 620 and 328 bp, respectively.

*Cell proliferation assay*. Cell proliferation of chondrocytes was assessed using the *in vivo* bromodeoxyuridine (BrdU) assay as previously described (21). Briefly, mice were intraperitoneally injected with 25 $\mu$l/25 g body weight BrdU at P3 and P5. The animals were then euthanized at P8, P14, and P21 for specimen collection followed by immunohistochemistry (22).

*Histology*. After the animals were euthanized at P8, P14, and P21, their right knee joints (n=3) were harvested and immersed in 10% formalin for 72 h at room temperature. The specimens were processed without decalcification and embedded in a single block of Paraplast X-tra (Thermo Fisher Scientific, Inc.). Thereafter, 6-$\mu$m coronal sections were mounted on slides. Safranin O/Fast green staining for 2 h at room temperature was performed to evaluate the developmental growth plate and hypertrophic differentiation at P8 and P21, whereas Von Kossa staining for 2 h at room temperature was used to evaluate tissue

mineralization at P8 and P14. Photomicrographs were obtained using a Nikon Ri1 microscope (Nikon Corporation) (23,24).

*Whole-body staining and skeletal analysis*. The mice were euthanized before the experiment began. The mineralization pattern of the skeleton was analyzed at P10 using whole-body staining as previously described (25). Briefly, mice were skinned under anesthesia, eviscerated and fixed in 95% ethanol for 1-2 days. Subsequently, acetone was used to remove fat. Skeletons were stained using Alizarin red S/Alcian blue for 3 days at 37˚C and sequentially immersed in 1% aqueous KOH at room temperature until the skeletons were clearly visible. Mineralized bones were visualized through the staining (23).

*Microcomputed tomography (μCT)*. Three tibial tissues isolated from each group (8-day old mice) were fixed in 70% ethanol for 24 h at room temperature and prepared for high resolution μCT (SkyScan 1172). Images were obtained using the following parameters: 40 kV, 80 μA, Pixel size=8.5 μm, 2,000x1,332 matrix, six averages and a 0.5-mm aluminum filter. Images were reconstructed using a threshold of 0-0.09, beam hardening correction of 35, ring artifact correction of 7 and Gaussian smoothing (factor=1). From the reconstructed images of the tibia, the 637-μm region immediately proximal to the growth plate was examined for the trabecular bone. The volume images of each group were analyzed using CTAn software (v1.7.1, SkyScan, Burker) to determinate the trabecular bone microstructure and trabecular thickness (Tb.Th), trabecular separation (Tb.Sp).

*Immunohistochemistry*. BrdU and proliferating cell nuclear antigen (PCNA) are typical proliferation markers that can indicate the proliferative activity of chondrocytes. BrdU is a synthetic nucleoside used to detect cellular proliferation by incorporating the place of thymine and pairs with guanine (26). PCNA is a multifunctional protein present in the nuclei of eukaryotic cells and has a crucial role in DNA replication and DNA repair systems (27). Matrix metalloproteinase (MMP)-13 is marker associated with endochondral ossification and bone repair (28). Runx2 and osteoprotegerin (OPG) are typical mineralization markers. Runx2 is a transcription factor essential for osteoblast differentiation and chondrocyte maturation (29). OPG is a key protective factor of bony tissue and is responsible for osteoclast formation and postnatal bone growth (30). To determine the expressions of these markers, 6-μm coronal sections of right knee joints were placed on positively charged glass slides (Thermo Fisher Scientific, Inc.). The sections were dried on a hotplate to increase tissue adherence. Immunohistochemistry was performed using the 3,3'diaminobenzidine (DAB), streptavidin-peroxidase (SP) and the DAB Histostain-SP immunohistochemistry kit (Zymed; Thermo Fisher Scientific, Inc.). Sections were deparaffinized and rehydrated using xylene and an alcohol gradient. Endogenous peroxidase was blocked by treating the sections with 3% hydrogen peroxide in methanol (Sigma-Aldrich; Merck KGaA) for 30 min at room temperature. The sections were then digested with 5 mg/ml hyaluronidase in phosphate-buffered saline (PBS) (Sigma-Aldrich; Merck KGaA) for 20 min and incubated with specific antibodies against MMP-13 (1:500, cat. no. ab219620, Abcam), BrdU (1:100, cat. no. ab8955, Abcam), PCNA (1:10,000, cat. no. ab29, Abcam), Runx2 (1:1,000, cat. no. 192256, Abcam), OPG (1:100, cat. no. 203061, Abcam) and CD34 (1:2,500, cat. no. 81289, Abcam) at 4˚C overnight. After treatment with biotinylated secondary antibody and SP conjugate (500 μl, Histostain®-Plus 3rd Gen IHC Detection kit, cat. no. D859673, Zymed; Thermo Fisher Scientific, Inc.) at 37˚C for 30 min, the sections were developed in DAB chromogen (Zymed; Thermo Fisher Scientific, Inc.) and then counterstained with hematoxylin (Zymed; Thermo Fisher Scientific, Inc.) for 2 min at room temperature. Images were captured using a Nikon Ri1 light microscope (Nikon Corporation) at x4 magnification. Percentages of positive staining for BrdU, PCNA, MMP-13, Runx2, OPG and CD34 in both the groups were semi quantified using the Image-Pro Plus 7.0 software (Media Cybernetics, Inc.) as described previously (31). Mean values from three independent measurements were used for statistical analysis (n=3).

*In situ hybridization (ISH)*. ISH was used to determine type X collagen (ColX) and Wnt5a expression levels as an indicator of HDAC4-downregualtion. ColX is a critical marker that represents terminal differentiation during chondrogenesis (32). Wnt5a a member of Wnt family that plays a vital role in regulating skeletal development (33). ISH was performed on paraffin sections prepared from tibial tissues at P8 as described previously (34). Accordingly, 10-μm sections were placed on positively charged glass slides (Thermo Fisher Scientific, Inc.) and subsequently dried on a hotplate to increase tissue adherence. These sections were then deparaffinized and rehydrated using conventional methods. Briefly, the tibial sections were incubated with proteinase K (cat. no. P8107S; New England BioLabs, Inc.) at 60˚C for 15 min and then rinsed with diethyl pyrocarbonate (DEPC)-PBS for 5 min. Thereafter, the tibial sections were incubated with 5 mg/ml hyaluronidase at 37˚C for 15 min and then rinsed with DEPC-PBS for 5 min. The sections were prehybridized for 1 h and hybridized for 16 h with a 0.5-μl probe (Col X and Wnt5a, from Department of Orthopedics, The Warren Alpert Medical School of Brown University) at 50˚C. The sections were washed with 5X saline sodium citrate (SSC) for 5 min at room temperature and 4X SSC for 30 min at 50˚C. Thereafter, the tibial sections were incubated with Tris-HCL-NaCl-EDTA buffer at 37˚C for 10 min; washed with 2XSSC for 10 min, 0.2XSSC for 10 min and 0.1XSSC buffer for 10 min. Following this, the sections were incubated with a blocking buffer for 1 h at room temperature. Digoxin antibody (1:200, ca. no. ab420, Abcam) was added to the sections for 2 h at room temperature. The reaction was stopped with tris-EDTA (TE) buffer (pH 8.0) for 10 min. The sections were then washed with distilled water and counterstained with hematoxylin (Zymed; Thermo Fisher Scientific, Inc.) for 2 min at room temperature. Images were captured using a Nikon Ri1 light microscope (Nikon Corporation) at x4 magnification.

*Reverse transcription-quantitative (RT-q)PCR*. The mRNA levels of *HDAC4*, *PCNA*, *MMP-13*, *Runx2*, *OPG* and osteocalcin were quantified using RT-qPCR. Total RNA was isolated using TRIzol (Life Technologies; Thermo Fisher Scientific, Inc.) from the sternum cartilage using the RNeasy isolation kit (Qiagen, Inc.). Accordingly, 1 μg total RNA was

reverse transcribed into cDNA using the iScripTM cDNA synthesis kit (Bio-Rad Laboratories, Inc.), with reaction conditions: 25˚C 5 min, 42˚C for 30 min, 85˚C for 5 min and kept at 4˚C. Thereafter, 50 ng/$\mu$l of the resulting cDNA was used as the template to quantify the relative mRNA content using the QuantiTect SYBR Green PCR kit (Qiagen, Inc.) with the DNA Engine Opticon 2 Continuous Fluorescence Detection system (MJ Research; Bio-Rad Laboratories, Inc.). qPCR was initiated for 30 sec at 94˚C, then 40 cycles of denaturation at 9˚C for 30 sec, primer annealing for 3 sec at 60˚C and a final extension step at 72˚C for 30 sec. Primer pairs that were used for quantitative detection of gene expression are listed in Table I, and 18S rRNA was used as the internal control. The cycle threshold values for target genes were measured and calculated using a computer software (MJ Research; Bio-Rad Laboratories, Inc.). Relative transcript levels were calculated using the $2^{-\Delta\Delta Cq}$ method where $\Delta\Delta$Cq=$\Delta$Cq E-$\Delta$Cq C, $\Delta$Cq E=Cqexp-Cq18S, and $\Delta$Cq C=CqCCq 18S (35).

*Statistical analysis*. Data from at least three separate experiments are presented as mean ± standard deviation. Differences between groups were analyzed using unpaired t-tests and $P<0.05$ was considered to indicate a statistically significant difference. Statistical analyses were performed using SPSS software v18.0 (SPSS Inc.).

Table I. Primer sequences for reverse transcription-polymerase chain reaction.

| Mouse gene | Primer sequence, 5'-3' |
|---|---|
| *HDAC4* | |
| Forward | ATCTGCCCACCAGAGTATGTG |
| Reverse | CTTGTTGAGAACAAACTCCTGCAGCT |
| *MMP-13* | |
| Forward | GGACCTTCTGGTCTTCTGGC |
| Reverse | GGATGCTTAGGGTTGGGGTC |
| *Runx2* | |
| Forward | CCGCACGCAAACCGCACCAT |
| Reverse | CGCTCCGGCCCACAAATCTC |
| *PCNA* | |
| Forward | GCCGAGATCTCAGCCATATT |
| Reverse | ATGTACTTAGAGGTACAAAT |
| *OPG* | |
| Forward | ATTGGCTGAGTGTTTTGGTGG |
| Reverse | CGCTGCTTTCACAGAGGTCA |
| Osteocalcin | |
| Forward | ATGAGAGCCCTCAGACTCCTC |
| Reverse | CGGGCCGTAGAAGCGCCGATA |
| 18s rRNA | |
| Forward | CGGCTACCACATCCAAGGAA |
| Reverse | CGCTCCGGCCCACAAATCTC |

## Results

*Generation of HDAC4, Col2α1-Cre mice*. To investigate the function of HDAC4 *in vivo*, the mouse *HDAC4* gene was deleted using homologous combination. The targeting strategy is presented in Fig. 1A. Wild-type, homologous and heterozygous mice were confirmed using qPCR. Product sizes for wild-type *HDAC4*, floxed and Cre alleles were 480, 620 and 328 bp, respectively (Fig. 1B). The HDAC4$^{d/d}$, Col2α1-Cre mice survived until P21, were severely runted and smaller compared with HDAC4$^{fl/fl}$ mice at P2, P4, P6 and P8 (Fig. 1C). These results indicated that the development of HDAC4$^{d/d}$, Col2α1-Cre mice was slower compared with that of HDAC4$^{fl/fl}$ mice.

*Shortened growth plates and disordered hypertrophic chondrocyte zones in HDAC4$^{d/d}$, Col2α1-Cre mice*. Chondrocyte hypertrophy is widely observed in endochondral ossification (5). During bone formation, chondrocytes were enlarged, and they secreted more ColX compared with the early stage of the ossification (5). Here, Safranin O/Fast green staining was performed on paraffin sections from HDAC4$^{fl/fl}$ and HDAC4$^{d/d}$, Col2α1-Cre mice at P8 (femur and tibia) (Fig. 2A-C) and P21 (tibia; Fig. 2D). As shown in Fig. 2A2-C2 and Fig. 2A4-C4, HDAC4$^{d/d}$, Col2α1-Cre mice had fewer prehypertrophic and hypertrophic chondrocyte zones compared with the HDAC4$^{fl/fl}$ mice (Fig. 2A1-C1 and A3-C3) at P8. In addition, the hypertrophic chondrocyte zone appeared smaller, and chondrocytes underwent degradation in the HDAC4$^{d/d}$, Col2α1-Cre mice group (Fig. 2A2-C2 and A4-C4) compared with the HDAC4$^{fl/fl}$ mice (Fig. 2A1-C1 and A3-C3) at P8. As presented in Fig. 2D-2, HDAC4$^{d/d}$, Col2α1-Cre mice showed decreased proteoglycans zones (marked by yellow arrows), premature ossification (marked by black arrows) compared with the HDAC4$^{fl/fl}$ mice (Fig. 2D-1) at P21. These results indicated that the shortened growth plates and disordered hypertrophic chondrocyte zones in HDAC4$^{d/d}$, Col2α1-Cre mice compared with that of HDAC4$^{fl/fl}$ mice.

*Accelerated vascular invasion and mineralization due to HDAC4-knockout*. During hypertrophic chondrocyte mineralization, blood vessels are induced by hypertrophic chondrocytes that secreted vascular endothelial growth factor (36). Von Kossa staining was performed to assess mineralization and vascular invasion of the tissue in HDAC4$^{fl/fl}$ mice and HDAC4$^{d/d}$, Col2α1-Cre mice at P8 (Fig. 3A and B) and P14 (Fig. 3C and D). As encircled in Fig. 3B1, vascular invasion of the growth plates in HDAC4$^{d/d}$, Col2α1-Cre mice began to appear at P8, whereas HDAC4$^{fl/fl}$ mice had no vascular formation at P8 (Fig. 3A1). More importantly, HDAC4$^{d/d}$, Col2α1-Cre mice developed an earlier secondary center of ossification (red circled area) and growth plates (yellow circled area; Fig. 3D and D1) compared with HDAC4$^{fl/fl}$ mice (Fig. 3C and C1) at P14. Moreover, the HDAC4$^{d/d}$, Col2α1-Cre mice had thicker cortical (Fig. 3D2) and cancellous bones (Fig. 3D3) compared with HDAC4$^{fl/fl}$ mice (Fig. 3C2 and C3). These results indicated that the vascular invasion and mineralization were accelerated in HDAC4$^{d/d}$, Col2α1-Cre mice compared with HDAC4$^{fl/fl}$ mice.

*Abnormal and premature mineralization due to HDAC4 deletion*. The detailed skeletal phenotypes of the HDAC4$^{fl/fl}$ and HDAC4$^{d/d}$, Col2α1-Cre groups were

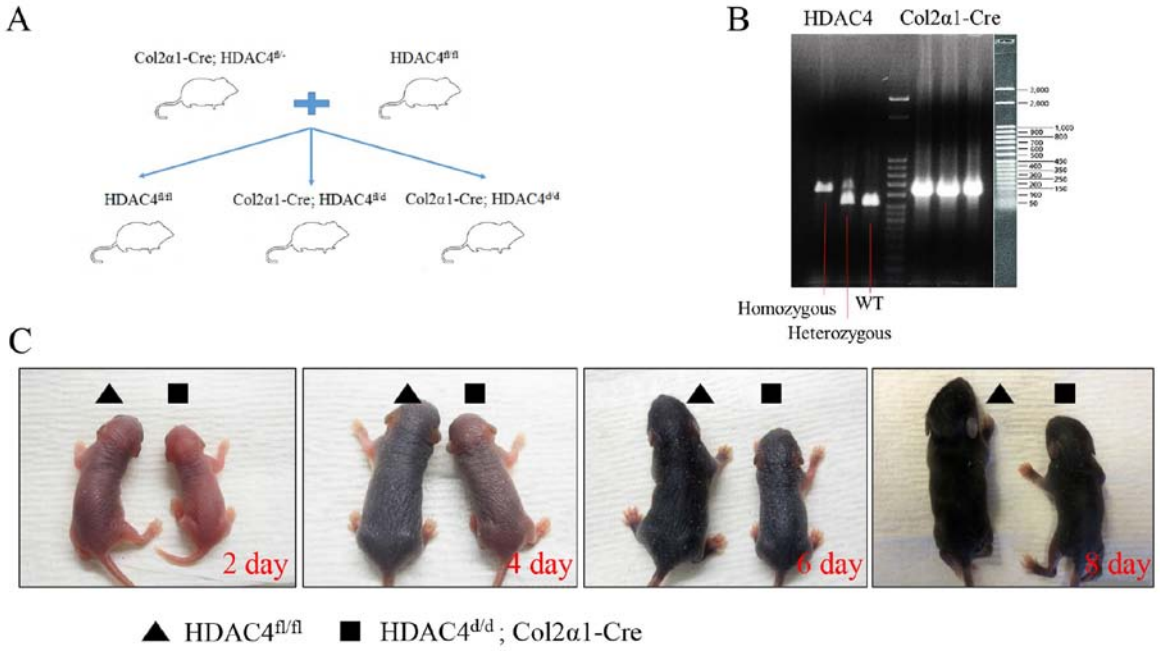


Figure 1. Generation of HDAC4, Col2α1-Cre mice. (A) Mating of HDAC4$^{fl/-}$, Col2α1-Cre and HDAC4$^{fl/fl}$ mice. (B) Representative PCR results of genomic DNA from wild-type and *HDAC4* heterozygous and homozygous null animals. (C) Images of the HDAC4$^{fl/fl}$ and HDAC4 $^{d/d}$, Col2α1-Cre offspring at postnatal days 2, 4, 6 and 8. HDAC4, histone deacetylase 4; Col2α1, collagen type 2α1; fl, floxed; d, down.

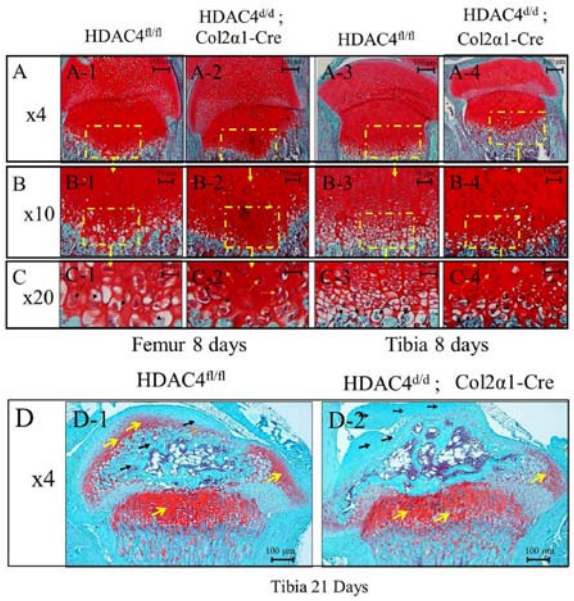


Figure 2. Safranin O/Fast green staining on paraffin sections of the femur and tibia tissues at P8 and P21. (A-C) Safranin O/Fast green staining showing femur and tibia tissue sections (magnification, x4, x10 and x20 respectively) at P8. The HDAC4$^{d/d}$, Col2α1-Cre mice had fewer cartilage tissues in the hypertrophy zone at P8 compared with those in the HDAC4$^{fl/fl}$ mice. Black arrows represent hypertrophic chondrocytes, and orange arrows represent chondrocytes degradation. Scar bars, 100 or 50 $\mu$m. (D) Safranin O/Fast green staining showing tibia tissue sections (magnification, x4) at P21. The HDAC4$^{d/d}$, Col2α1-Cre mice had fewer proteoglycans but more ossification at P21 compared with the HDAC4$^{fl/fl}$ mice. The yellow arrow represents zone of proteoglycans, the black arrow represents zone of ossification, Scale bars, 100 $\mu$m. P, postnatal day; HDAC4, histone deacetylase 4; Col2α1, collagen type 2α1; fl, floxed; d, down.

analyzed using Alizarin red and Alcian blue staining at P10 (Fig. 4A and B). Alizarin red and Alcian blue staining of the whole skeleton of HDAC4$^{d/d}$, Col2α1-Cre mice revealed obvious malformed and premature mineralization of the endochondral skeleton, including the sternum (Fig. 4D), xiphisternum (Fig. 4D), tibia (Fig. 4F) and intervertebral disk (Fig. 4H) compared with HDAC4$^{fl/fl}$ mice(Fig. 4C, E and G). Ectopic ossification of the endochondral cartilage prevented normal expansion of the rib cage (Fig. 4D) $\mu$CT analysis showing the HDAC4$^{d/d}$, Col2α1-Cre mice (Fig. 4J) have more cancellous bone than HDAC4$^{fl/fl}$ mice (Fig. 4I) at P8. The Tb.Th was significantly greater in the HDAC4$^{d/d}$, Col2α1-Cre mice compared with HDAC4$^{fl/fl}$ mice, as measured by $\mu$CT ($P<0.05$; Fig. 4K). Simultaneously, Tb.Sp was significantly reduced in the HDAC4$^{d/d}$, Col2α1-Cre mice compared with that in HDAC4$^{fl/fl}$ mice ($P<0.05$; Fig. 4L). These results indicated that abnormal and premature mineralization occurs in the knockout mouse.

*Decreased chondrocyte proliferation due to HDAC4 deletion via Wnt5a signaling pathway inhibition and increased chondrocyte hypertrophy.* Immunohistochemistry was performed to determine the presence of BrdU, PCNA, MMP-13, Runx2, OPG and CD34 in HDAC4$^{fl/fl}$ and HDAC4$^{d/d}$, Col2α1-Cre mice (Fig. 5A-L). The percentages areas positively expressing MMP-13, Runx2, OPG and CD34, were significantly higher in the HDAC4$^{d/d}$, Col2α1-Cre mice compared with the HDAC4$^{fl/fl}$ mice (all $P<0.05$; Fig. 5M-R). Conversely, the expressions of typical proliferative markers, including BrdU and PCNA, were significantly lower in the HDAC4$^{d/d}$, Col2α1-Cre group compared with the HDAC4$^{fl/fl}$ group ($P<0.05$; Fig. 5M-R). ISH confirmed increased ColX and decreased Wnt5a expression (red boxes and arrows) in the HDAC4$^{d/d}$, Col2α1-Cre mice (Fig. 5S-Z). These results indicated that HDAC4 deletion reduce chondrocyte proliferation via Wnt5a signaling pathway inhibition and increased chondrocyte hypertrophy.

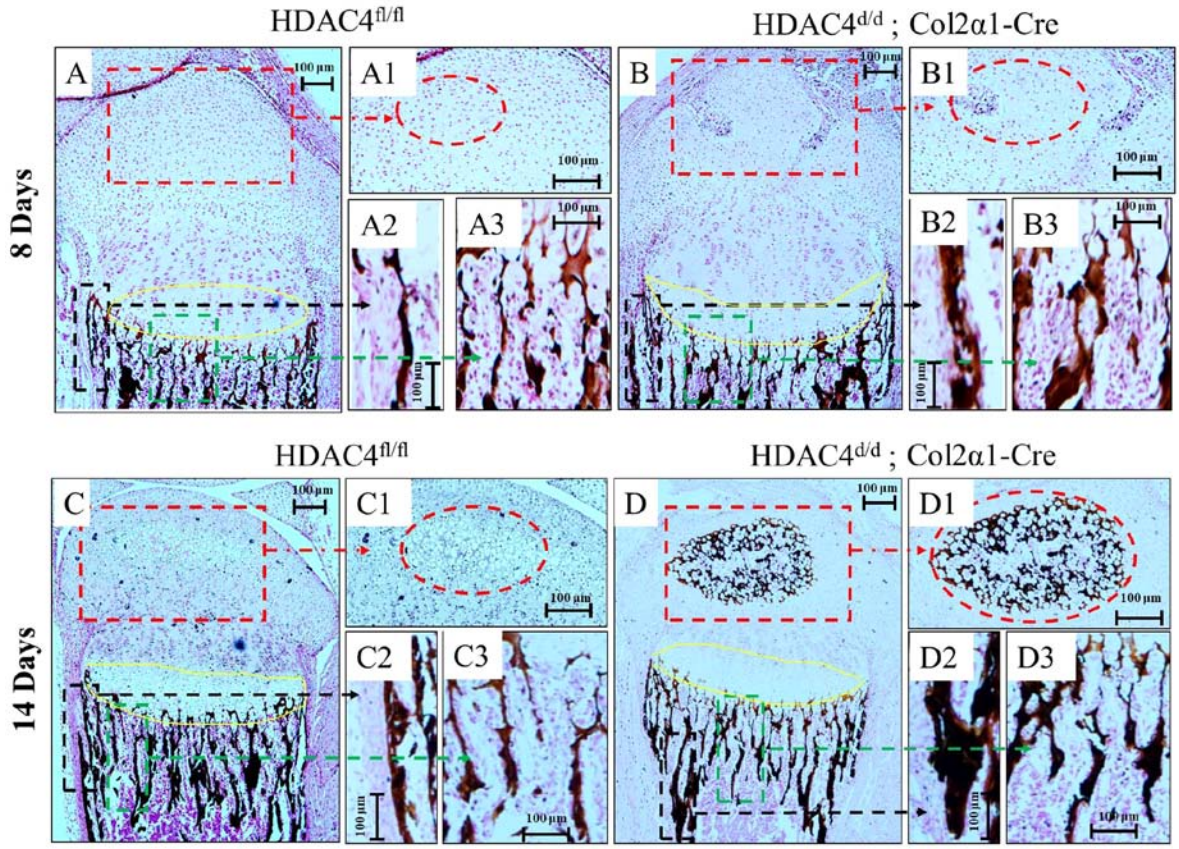


Figure 3. Mineralization and vascular invasion of tissues at (A and B) P8 and (C and D) P14 using Von Kossa staining. (B1, the red circled regions) vascular invasion and (D1, the red circled regions) secondary center of ossification were observed earlier in the HDAC4$^{d/d}$, Col2α1-Cre mice compared with in HDAC4$^{fl/fl}$ mice (A1 and C1, the red circled regions). The HDAC4$^{d/d}$, Col2α1-Cre mice had (B2 and D2) thicker cortical and (B3 and D3) cancellous bones compared with the (A2, C2, A3 and C3) HDAC4$^{fl/fl}$ mice. Yellow circled areas represent growth plates. Black circled areas represent cortical bones. Green circled areas represent cancellous bones. Boxes indicate area magnified in adjacent figures. Scale bars, 100 $\mu$m. P, postnatal day; HDAC4, histone deacetylase 4; Col2α1, collagen type 2α1; fl, floxed; d, down.

*Genetic changes associated with increased hypertrophy and mineralization and decreased proliferation in HDAC4$^{d/d}$, Col2α1-Cre mice*. qPCR analyses indicated that the mRNA levels of *HDAC4* and *PCNA* were lower and those of *MMP-13*, *Runx2*, *OPN* and osteocalcin were higher in the HDAC4$^{d/d}$, Col2α1-Cre mice compared with those of HDAC4$^{fl/fl}$ mice (all $P<0.05$; s. 6A-F). These results indicated that there are genetic changes associated with increased hypertrophy and mineralization and decreased proliferation in HDAC4$^{d/d}$, Col2α1-Cre mice.

## Discussion

The deletion of *HDAC4* results in precocious lethality in mice (9); however, the mechanism underlying HDAC4-mediated postnatal regulation of growth plate development remains unclear. A previous study demonstrated that HDAC4 is a critical negative regulator of chondrocyte hypertrophy due its binding to and inhibition of Runx2 (37). To further investigate the role of chondrocyte-derived HDAC4 in postnatal skeletal development, the present study selectively ablated the *HDAC4* gene in collagen type 2-expressing cells using the *Cre/loxP* gene targeting technique.

The findings of the current study demonstrated that *HDAC4*-deletion in Col2α1-expressing cells results in severely runted and slow-growing mice postdelivery, which is consistent with the result reported by a previous study (9). In addition, the expressions of typical proliferative markers BrdU and PCNA were significantly lower in the HDAC4$^{d/d}$, Col2α1-Cre mice compared with in their HDAC4$^{fl/fl}$ control littermates, which suggested HDAC4-deletion is associated with decreased chondrocyte growth. ISH demonstrated that the HDAC4$^{d/d}$, Col2α1-Cre mice had a downregulated expression of Wnt5a compared with that in the HDAC4$^{fl/fl}$ mice. Recent studies have also reported that Wnt signaling is one of the numerous signaling pathways involved in the regulation of diverse processes underpinning fundamental and normal development, such as apoptosis, proliferation, differentiation and polarity (38,39).

*Wnt5a*-knockout mice demonstrate perinatal lethality primarily due to respiratory failure and presented extensive developmental abnormalities (15). Wnt5a and its signaling pathway can regulate fundamental cellular processes, including proliferation and survival. These results suggest that Wnt5a is a potential target for treating proliferation-related diseases (40). The present findings suggested that *HDAC4*-deletion results in decreased chondrocyte proliferation partially due to the inhibition of Wnt5a expression.

The HDAC4$^{d/d}$, Col2α1-Cre mice exhibited premature and disordered hypertrophic chondrocytes as well as increased levels of MMP-13 and type X collagen. MMP-13 and collagen

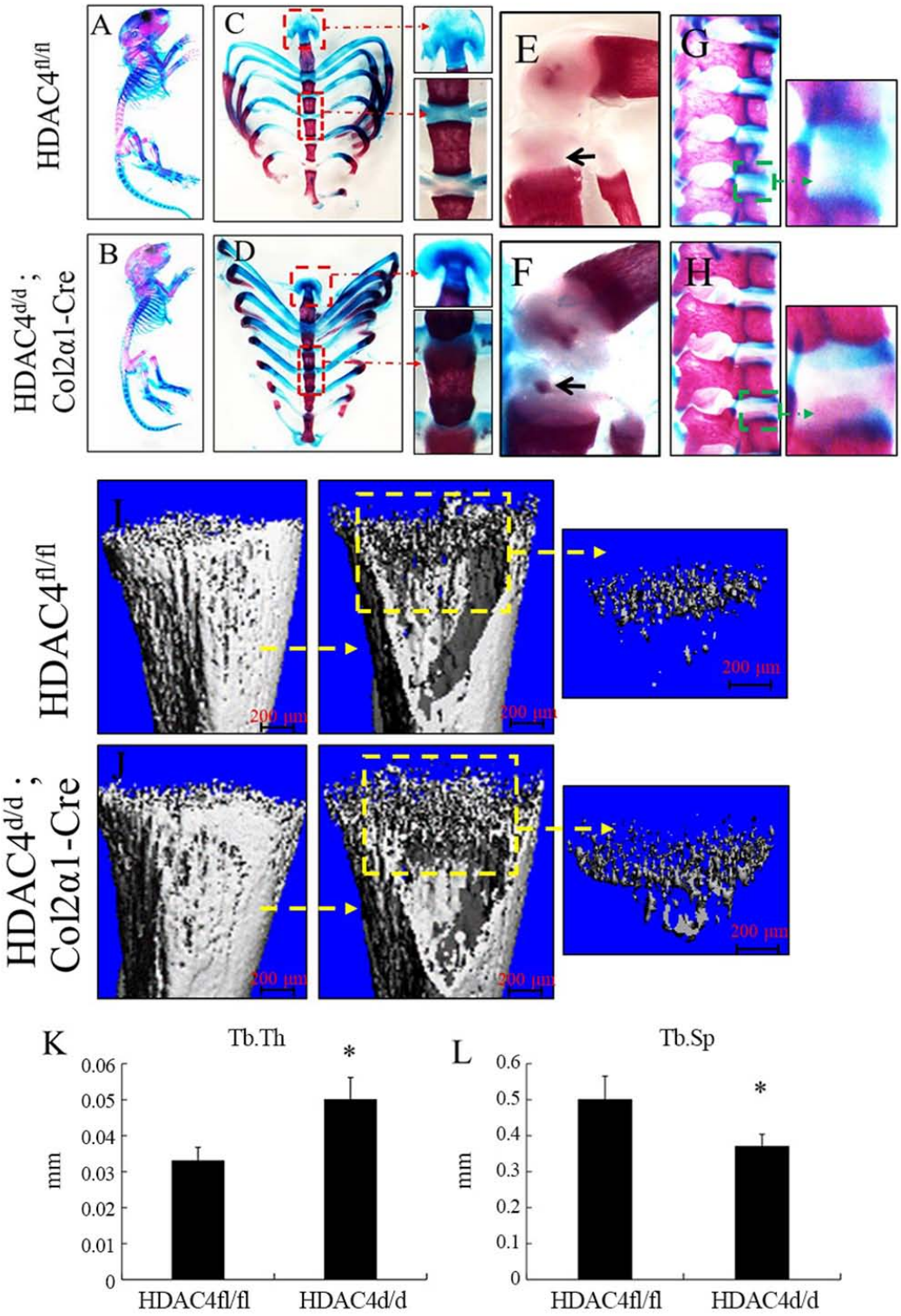


Figure 4. Premature ossification in HDAC4$^{d/d}$, Col2α1-Cre mice. (A-H) Alizarin red and Alcian blue stained skeletons of the HDAC4$^{fl/fl}$ and HDAC4$^{d/d}$, Col2α1-Cre mice at P10, the red boxes and arrow represent xiphoid process and sternum, the green boxes and arrow represent lumbar vertebrae, black arrows represent tibia cartilage. (I and J) $\mu$CT analysis showing the bone image of tibial tissues from the HDAC4$^{fl/fl}$ and the HDAC4$^{d/d}$, Col2α1-Cre mice at P8, yellow boxes and arrow represent cancellous bone. (K and L) Tb.Th, trabecular thickness; Tb.Sp, trabecular separation.in the HDAC4$^{fl/fl}$ and HDAC4$^{d/d}$, Col2α1-Cre mice were evaluated using $\mu$CT analysis. Each assay was performed in triplicates for each group. Scale bars, 200 $\mu$m. $^{*}$P<0.05 vs. HDAC4$^{fl/fl}$ mice. P, postnatal day; HDAC4, histone deacetylase 4; Col2α1, collagen type 2α1; fl, floxed; d, down; Tb.Th, trabecular thickness; Tb.Sp, trabecular separation.

type X are essential for maintaining chondrocyte hypertrophy and allowing ossification (41,42). It is universally accepted that hypertrophic chondrocytes implicate the final step in the maturation process of chondrocytes, which eventually results in apoptosis of chondrocytes and replacement of hypertrophic chondrocytes by bone tissues (43). Ossification begins when hypertrophic chondrocytes undergo programmed cell death, and the calcified cartilage is invaded by blood vessels,

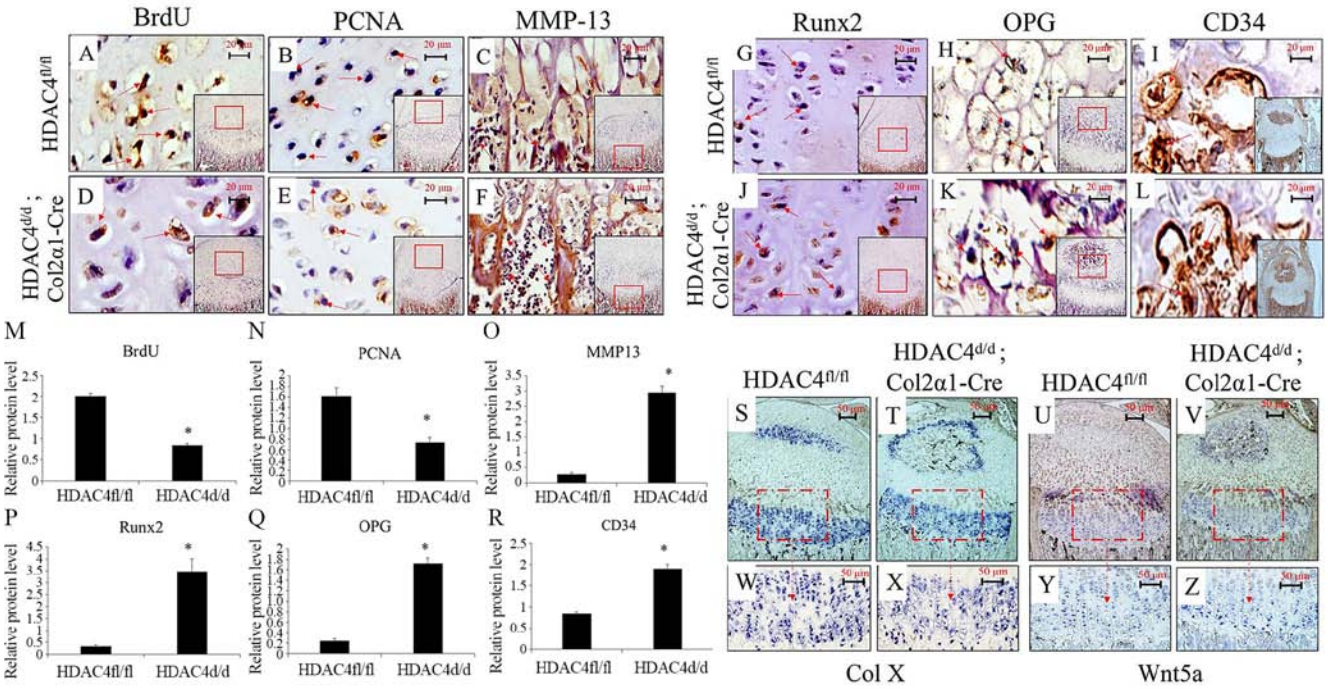


Figure 5. Decreased chondrocyte proliferation due to *HDAC4* deletion. (A-L) Immunohistochemical staining of the tibial articular cartilage of HDAC4$^{fl/fl}$ and HDAC4$^{d/d}$, Col2α1-Cre mice at P8 for determining the expressions of BrdU, PCNA, MMP-13, Runx2, OPG. and CD34 Positive signals (brown staining) are indicated by red arrows. Scale bars, 20 $\mu$m. (M-R) Semiquantitative analysis of positively expressed areas for BrdU, PCNA, MMP-13, Runx2, OPG and CD34. (S-Z) *In situ* hybridization on paraffin sections prepared for determining the expressions of Col X and Wnt5a in tibial tissues at P14. The HDAC4$^{d/d}$, Col2α1-Cre mice had decreased expressions of BrdU, PCNA and Wnt5a but increased expressions of MMP-13, Runx2, OPG, Col X and CD34. Boxed areas in S-V indicate the regions shown in W-Z, respectively. Scale bars, 50 $\mu$m. $^{*}$P<0.05 vs. HDAC4$^{fl/fl}$ mice. P, postnatal day; HDAC4, histone deacetylase 4; Col2α1, collagen type 2α1; fl, floxed; d, down; BrdU, bromodeoxyuridine; PCNA, proliferating cell nuclear antigen; MMP-13, matrix metalloproteinase-13; Runx2, runt-related transcription factor 2; Col X, type X collagen; OPG, osteoprotegerin.

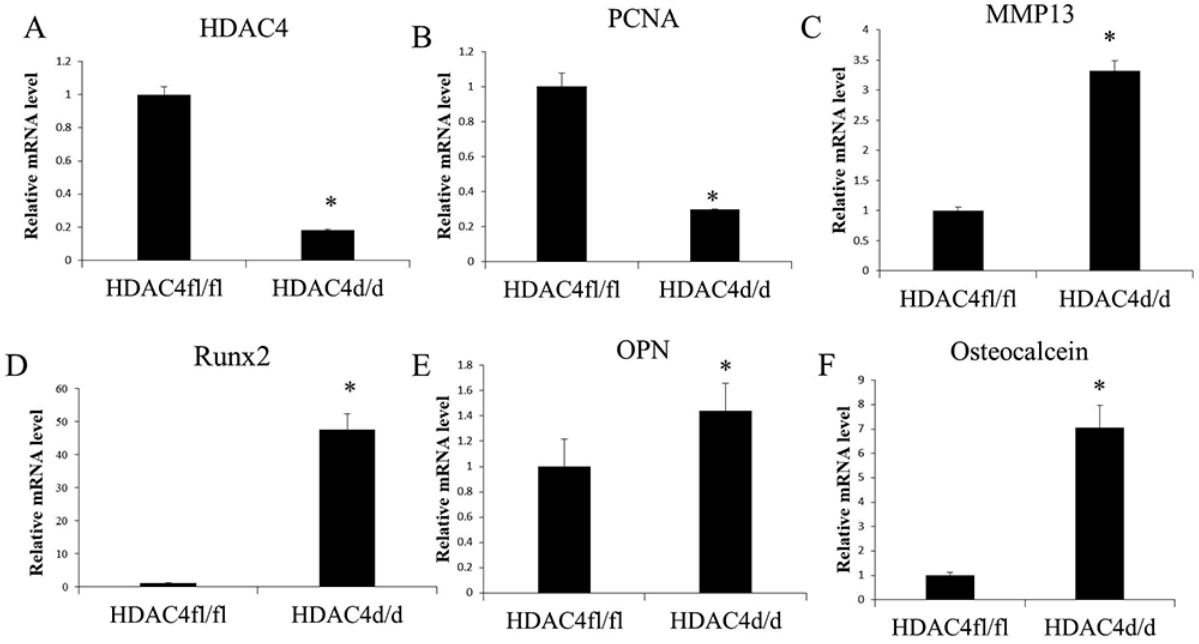


Figure 6. Reverse transcription quantitative-PCR was used to analyze the mRNA levels of (A) *HDAC4*, (B) *PCNA*, (C) *MMP-13*, (D) *Runx2*, (E) *OPN* and (F) osteocalcin in HDAC4$^{d/d}$, Col2α1-Cre and HDAC4$^{fl/fl}$ mice from three independent experiments. n=3. $^{*}$P<0.05 vs. control. HDAC4, histone deacetylase 4; Col2α1, collagen type 2α1; fl, floxed; d, down; PCNA, proliferating cell nuclear antigen; MMP-13, matrix metalloproteinase-13; Runx2, runt-related transcription factor 2; OPG, osteoprotegerin.

osteoblasts, osteoclasts and mesenchymal precursors, thereby forming primary and secondary ossification centers (3,4). The degradation and remodeling of the cartilage matrix is necessary for vascular invasion, whereas angiogenesis has been implicated as a crucial step in endochondral ossification (5). The present study identified that *HDAC4* gene ablation

can accelerate the mineralization and ectopic ossification of endochondral cartilages. The expressions of typical mineralization markers, including Runx2, OPN and osteocalcin, were increased in the HDAC4$^{d/d}$, Col2α1-Cre mice. Therefore, it was hypothesized that premature and disordered chondrocyte hypertrophy in *HDAC4*-knockout mice accelerates the malformation of bones and results in runted mice.

Notably, the vascular invasion and secondary center of ossification of the growth plates began to appear at P8 in the HDAC4$^{d/d}$, Col2α1-Cre mice, whereas that in the control group began to appear at P14. Vascular invasion of the primarily avascular hypertrophic chondrocyte zone of the growth plate is a prerequisite for endochondral bone formation and occurs in a sequence of events (44). Blood vessels supplying bones orchestrate the process of bone development and remodeling as well as regulate skeleton regeneration by delivering nutrients, oxygen, hormones or growth factors to bone cells (45). This process requires a dynamic and close interaction between hypertrophic chondrocytes and vascular invasion. The expressions of typical vascular formation markers, such as CD34 (a widely used marker of hematopoietic and endothelial progenitor cells), were reportedly increased in the tibia of the HDAC4$^{d/d}$, Col2α1-Cre mice (46). The findings of the present study demonstrated that knockout of the *HDAC4* gene accelerates endochondral bone formation by promoting vascular invasion.

There are some limitations in this experiment. The number of animals was small and no cell experiment was conducted. More research is needed on the HDAC4 pathway and in the future Wnt5a loss and gain of function studies *in vitro* and *in vivo* should be performed to confirm the regulating effect of the HDAC4-Wnt5a pathway. HDAC4-Wnt5a-β-catenin signaling activity should be analyzed as it is speculated that HDAC4-Wnt5a-β-catenin may be an indispensable role in the homeostasis of articular cartilage (47). In the present study, the HDAC4$^{d/d}$, Col2α1-Cre mice displayed a marked phenotype characterized by decreased chondrocyte hypertrophy, early blood invasion and premature bone formation, leading to abnormal growth and runted mice. These results demonstrated that chondrocyte-derived HDAC4 is primarily responsible for the regulation of chondrocyte differentiation and endochondral bone formation.

## Acknowledgements

The authors would like to thank Dr Olson (University of Texas Southwestern Medical Center) who provided the HDAC4$^{fl/fl}$ mice and technical support.

## Funding

The current study was supported by The National Institute of General Medical Sciences, National Institutes of Health (grant no. P30GM122732), RIH Orthopedic Foundation and The National Natural Science Foundation of China (grant no. 81704103, mainly used for the author's study expenses in the United States).

## Availability of data and materials

All data generated or analyzed during this study are included in this published article.

## Authors' contributions

LW and HZ designed the study. GD, CX and XS performed the experiments. YS, PL and XWe collected the experimental data. MZ, SW, LG, XWa and NW analyzed the experimental data. All authors read and approved the final manuscript.

## Ethics approval and consent to participate

The present study was approved by the Institutional Animal Care and Use Committee of Rhode Island Hospital.

## Patient consent for publication

Not applicable.

## Competing interests

The authors declare that they have no competing interests.

## References

1. Li J and Dong S: The signaling pathways involved in chondrocyte differentiation and hypertrophic differentiation. Stem Cells Int 2016: 2470351, 2016.
2. James CG, Stanton LA, Agoston H, Ulici V, Underhill TM and Beier F: Genome-wide analyses of gene expression during mouse endochondral ossification. PLoS One 5: e8693, 2010.
3. Mackie E, Ahmed YA, Tatarczuch L, Chen KS and Mirams M: Endochondral ossification: How cartilage is converted into bone in the developing skeleton. Int J Biochem Cell Biol 40: 46-62, 2008.
4. Mackie EJ, Tatarczuch L and Mirams M: The skeleton: A multi-functional complex organ: The growth plate chondrocyte and endochondral ossification. J Endocrinol 211: 109-121, 2011.
5. Sun MM and Beier F: Chondrocyte hypertrophy in skeletal development, growth, and disease. Birth Defects Res C Embryo Today 102: 74-82, 2014.
6. Zhang W, Chen J, Zhang S and Ouyang HW: Inhibitory function of parathyroid hormone-related protein on chondrocyte hypertrophy: The implication for articular cartilage repair. Arthritis Res Ther 14: 221, 2012.
7. Rim YA, Nam Y and Ju JH: The role of chondrocyte hypertrophy and senescence in osteoarthritis initiation and progression. Int J Mol Sci 21: 2358, 2020.
8. De Ruijter AJ, Van Gennip AH, Caron HN, Stephan KE and Van Kuilenburg AB: Histone deacetylases (HDACs): Characterization of the classical HDAC family. Biochem J 370: 737-749, 2003.
9. Vega RB, Matsuda K, Oh J, Barbosa AC, Yang X, Meadows E, McAnally J, Pomajzl C, Shelton JM, Richardson JA, *et al*: Histone deacetylase 4 controls chondrocyte hypertrophy during skeletogenesis. Cell 119: 555-566, 2004.
10. Nakatani T, Chen T, Johnson J, Westendorf JJ and Partridge NC: The deletion of hdac4 in mouse osteoblasts influences both catabolic and anabolic effects in bone. J Bone Miner Res 33: 1362-1375, 2018.
11. Nakatani T, Chen T and Partridge NC: MMP-13 is one of the critical mediators of the effect of HDAC4 deletion on the skeleton. Bone 90: 142-151, 2016.
12. Fu J, Li S, Feng R, Ma H, Sabeh F, Roodman GD, Wang J, Robinson S, Guo XE, Lund T, *et al*: Multiple myeloma-derived MMP-13 mediates osteoclast fusogenesis and osteolytic disease. J Clin Invest 126: 1759-1772, 2016.
13. Chen W, Sheng P, Huang Z, Meng F, Kang Y, Huang G, Zhang Z, Liao W and Zhang Z: MicroRNA-381 regulates chondrocyte hypertrophy by inhibiting histone deacetylase 4 expression. Int J Mol Sci 17: 1377, 2016.
14. Lories RJ, Corr M and Lane NE: To wnt or not to wnt: The bone and joint health dilemma. Nat Rev Rheumatol 9: 328-339, 2013.
15. Kikuchi A, Yamamoto H, Sato A and Matsumoto S: Wnt5a: Its signalling, functions and implication in diseases. Acta Physiol (Oxf) 204: 17-33,2012.

16. Wang Z, Qin G and Zhao TC: HDAC4: Mechanism of regulation and biological functions. Epigenomics 6: 139-150, 2014.
17. Huang HM, Li XL, Tu SQ, Chen XF, Lu CC and Jiang LH: Effects of roughly focused extracorporeal shock waves therapy on the expressions of bone morphogenetic protein-2 and osteoprotegerin in osteoporotic fracture in rats. Chin Med J (Engl) 129: 2567-2575, 2016.
18. Shahi M, Peymani A and Sahmani M: Regulation of bone metabolism. Rep Biochem Mol Biol 5: 73-82, 2017.
19. Long F, Zhang XM, Karp S, Yang Y and McMahon AP: Genetic manipulation of hedgehog signaling in the endochondral skeleton reveals a direct role in the regulation of chondrocyte proliferation. Development 128: 5099-5108, 2001.
20. American Veterinary Medical Association: AVMA Guidelines for the Euthanasia of Animals: 2013 Edition. Available at: https://www.avma.org/KB/Policies/Documents/euthanasia.pdf.
21. Zhao GZ, Zhang LQ, Liu Y, Fang J, Li HZ, Gao KH and Chen YZ: Effects of platelet-derived growth factor on chondrocyte proliferation, migration and apoptosis via regulation of GIT1 expression. Mol Med Rep 14: 897-903, 2016.
22. Estensoro I, Pérez-Cordón G, Sitjà-Bobadilla A and Piazzon MC: Bromodeoxyuridine DNA labelling reveals host and parasite proliferation in a fish-myxozoan model. J Fish Dis 41: 651-662, 2018.
23. Bourgine A, Pilet P, Diouani S, Sourice S, Lesoeur J, Beck-Cormier S, Khoshniat S, Weiss P, Friedlander G, Guicheux J and Beck L: Mice with hypomorphic expression of the sodium-phosphate cotransporter PiT1/Slc20a1 have an unexpected normal bone mineralization. PLoS One 8: e65979, 2013.
24. Zhang Z, Wei X, Gao J, Zhao Y, Zhao Y, Guo L, Chen C, Duan Z, Li P and Wei L: Intra-articular injection of cross-linked hyaluronic acid-dexamethasone hydrogel attenuates osteoarthritis: An experimental study in a rat model of osteoarthritis. Int J Mol Sci 17: 411, 2016.
25. Liu F, Fang F, Yuan H, Yang D, Chen Y, Williams L, Goldstein SA, Krebsbach PH and Guan JL: Suppression of autophagy by FIP200 deletion leads to osteopenia in mice through the inhibition of osteoblast terminal differentiation. J Bone Miner Res 28: 2414-2430, 2013.
26. Harris L, Zalucki O and Piper M: BrdU/EdU dual labeling to determine the cell-cycle dynamics of defined cellular subpopulations. J Mol Histol 49: 229-234, 2018.
27. Fan L, Bi T, Wang L and Xiao W: DNA-damage tolerance through PCNA ubiquitination and sumoylation. Biochem J 477: 2655-2677, 2020.
28. Wang M, Sampson ER, Jin H, Li J, Ke QH, Im HJ and Chen D: MMP13 is a critical target gene during the progression of osteoarthritis. Arthritis Res Ther 15: R5, 2013.
29. Komori T: Runx2, an inducer of osteoblast and chondrocyte differentiation. Histochem Cell Biol 149: 313-323, 2018.
30. Chen D, Liu Y, Liu Z and Wang P: OPG is required for the postnatal maintenance of condylar cartilage. Calcif Tissue Int 104: 461-474, 2019.
31. Eid AA, Lee DY, Roman LJ, Khazim K and Gorin Y: Sestrin 2 and AMPK connect hyperglycemia to Nox4-dependent endothelial nitric oxide synthase uncoupling and matrix protein expression. Mol Cell Biol 33: 3439-3460, 2013.
32. Roux CH, Pisani DF, Gillet P, Fontas E, Yahia HB, Djedaini M, Ambrosetti D, Michiels JF, Panaia-Ferrari P, Breuil V, *et al*: Oxytocin controls chondrogenesis and correlates with osteoarthritis. Int J Mol Sci 21: 3966, 2020.
33. Michigami T: Wnt signaling and skeletal dysplasias. Clin Calcium 29: 323-328, 2019 (In Japanese).
34. Han Q, Lin Q, Huang P, Chen M, Hu X, Fu H, He S, Shen F, Zeng H and Deng Y: Microglia-derived IL-1β contributes to axon development disorders and synaptic deficit through p38-MAPK signal pathway in septic neonatal rats. J Neuroinflammation 14: 52, 2017.
35. Livak KJ and Schmittgen TD: Analysis of relative gene expression data using real-time quantitative PCR and the 2(-Delta Delta C(T)) method. Methods 25: 402-408, 2001.
36. Zelzer E, Mamluk R, Ferrara N, Johnson RS, Schipani E and Olsen BR: VEGFA is necessary for chondrocyte survival during bone development. Development 131: 2161-2171, 2004.
37. Zhou J, Li P, Chen Q, Wei X, Zhao T, Wang Z and Wei L: Mitogen-activated protein kinase p38 induces HDAC4 degradation in hypertrophic chondrocytes. Biochim Biophys Acta 1853: 370-376, 2015.
38. Zhou Y, Kipps TJ and Zhang S: Wnt5a signaling in normal and cancer stem cells. Stem Cells Int 2017: 5295286, 2017.
39. Nusse R and Clevers H: Wnt/β-catenin signaling, disease, and emerging therapeutic modalities. Cell 169: 985-999, 2017.
40. Kumawat K and Gosens R: WNT-5A: Signaling and functions in health and disease. Cell Mol Life Sci 73: 567-587, 2016.
41. Bouaziz W, Sigaux J, Modrowski D, Devignes CS, Funck-Brentano T, Richette P, Ea HK, Provot S, Cohen-Solal M and Haÿ E: Interaction of HIF1α and β-catenin inhibits matrix metalloproteinase 13 expression and prevents cartilage damage in mice. Proc Natl Acad Sci USA 113: 5453-5458, 2016.
42. Nguyen L, Sharma A, Chakraborty C, Saibaba B, Ahn ME and Lee SS: Review of prospects of biological fluid biomarkers in osteoarthritis. Int J Mol Sci 18: 601, 2017.
43. Chen H, Ghori-Javed FY, Rashid H, Adhami MD, Serra R, Gutierrez SE and Javed A: Runx2 regulates endochondral ossification through control of chondrocyte proliferation and differentiation. J Bone Miner Res 29: 2653-2665, 2014.
44. Walzer SM, Cetin E, Grübl-Barabas R, Sulzbacher I, Rueger B, Girsch W, Toegel S, Windhager R and Fischer MB: Vascularization of primary and secondary ossification centres in the human growth plate. BMC Dev Biol 14: 36, 2014.
45. Filipowska J, Tomaszewski KA, Niedźwiedzki Ł, Walocha JA and Niedźwiedzki T: The role of vasculature in bone development, regeneration and proper systemic functioning. Angiogenesis 20: 291-302, 2017.
46. Hassanein S, Nasr Eldin MH, Amer HA, Abdelhamid AE, El Houssinie M and Ibrahim A: Human umbilical cord blood CD34-positive cells as predictors of the incidence and short-term outcome of neonatal hypoxic-ischemic encephalopathy: A pilot study. J Clin Neurol 13: 84-90, 2017.
47. Xuan F, Yano F, Mori D, Chijimatsu R, Maenohara Y, Nakamoto H, Mori Y, Makii Y, Oichi T, Taketo MM, *et al*: Wnt/β-catenin signaling contributes to articular cartilage homeostasis through lubricin induction in the superficial zone. Arthritis Res Ther 21: 247, 2019.